Some analysis of a two-dimensional double diffusion experiment

David Osmond

1 Introduction

Convection driven by double diffusion occurs when two properties contributing to the density of a fluid diffuse at different rates. In the ocean, the density of water is governed primarily by heat and salt, and the heat diffuses about 100 times faster than salt. It is now clear that double diffusion is an important process driving convection in the ocean, especially given its ability to move fluid particles across isopycnals.

Despite the primary mechanisms of double diffusion being formulated back in 1960 by Stern [1] as he considered the 'perpetual salt fountain' experiment conceived by his colleagues a few years earlier [2], there remains a great deal to be learnt on the subject. The two simplest examples of double diffusive convection are salt fingers and diffusive layers. Both types involve a stable stratification of one component, and an unstable stratification of the other, although the overall density field is always stable. Fingers occur when the faster diffusing component is stably stratified. If we consider the heat-salt situation present in oceans, salt fingers occur when the salt is unstably stratified, so there is hot salty water overlying cold fresh water. If a perturbation moves a fluid parcel downwards, it finds itself in cooler and fresher surroundings than was previously the case. It loses both heat and salt to the surrounding fluid; however, since temperature diffuses more rapidly, it experiences a net increase in density and thus continues its downwards motion. The surrounding fluid gains heat from this descending finger, and it in turn becomes lighter and moves upwards. Eventually the region becomes filled with fingers moving in alternating upwards and downwards directions.

Diffusive layers result when the slower diffusing substance is stably stratified. Thus in the ocean they occur when cool fresh water over lies hot salty water. Temperature diffuses faster than salt, so the bottom layer is heating the top layer, thus driving convection in a similar manner to Rayleigh Bénard convection. The top layer also cools the bottom, which also drives convection. The convection tends to homogenise the fluid above and below the diffusive interface so that a very sharp interface results.

These two processes are primarily one-dimensional. The substances in the mean state have gradients only in the vertical direction. The situation becomes more complicated when there are gradients in both horizontal and vertical planes, and the physics of this process are less well understood.

In 1996 Turner and Veronis resumed work on an experiment Turner had been considering for a long time, and which was designed to look at one example of the two-dimensional double

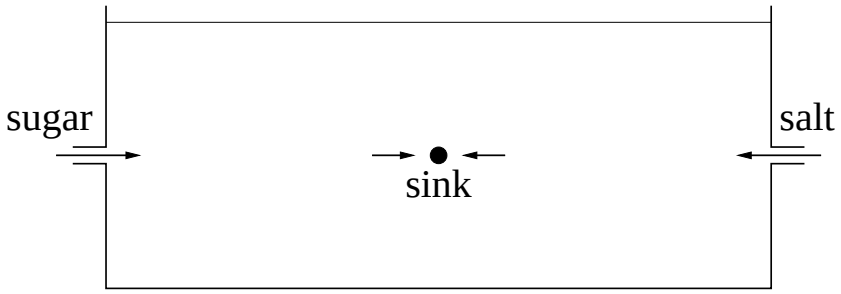

Figure 1: The experimental set-up. Salt and sugar are slowly pumped into the left and right hand side respectively of a long tank. Both source rates are 5 ml per minute. The volume of fluid in the tank is kept constant by using a constant head overflow device in the very center of the tank.

diffusive problem. Veronis' suggestion was to consider the simplest configurations possible, and here we consider one of them.

2 The Experiment

A long thin tank ($1820 \times 80 \times 120$ mm) is constructed with an inlet at the center of each end, and a constant pressure head outlet at mid height in the center of the tank. It is pictured in figure 1. The tank is filled with a 50-50 mixture of salt and sugar with a density $\rho = 1100$ kg/m^3. Sugar is chosen as the second diffusing component, as it does not diffuse through the side walls of the tank as does heat. Sugar has a diffusivity about 1/3 that of salt, and so in this system plays the role that salt does in the ocean, while the salt plays the part of heat in the real ocean.

The experiment commences by slowly pumping a salt solution with density $\rho = 1100$ kg/m^3 through the inlet at the left end of the tank, and a sugar solution with the same density in through the right hand inlet. Both flow rates are very close to 5 cm^3/min. Initially, when the salt emerges from the source at the left inlet, it is much saltier than the fluid in the tank, and thus salt diffuses out of it. Sugar also diffuses from the fluid in the tank into the salt plume, but at a slower rate. The plume gets lighter as salt diffuses from it, while a sheath of fluid surrounding the plume gets denser as the salt from the plume diffuses into it. Thus the plume separates into a light core which convects up towards the surface, and a dense sheath which sinks towards the base. The opposite process occurs at the sugar source, so that the core sinks and the sheath rises.

As time continues, the density difference between the the top and bottom of the tank increases. The rate of increase slows however, and after some time (a few days in this experiment), a steady state density field is formed. Active double diffusive convection still continues however, although it does not alter the density field significantly. To first order, the steady state convection consists of a region of fingering in the top left quadrant of the tank above the salt plume, and again in the lower right quadrant beneath the sugar source. In the top right and bottom left quadrants, diffusive layers are visible.

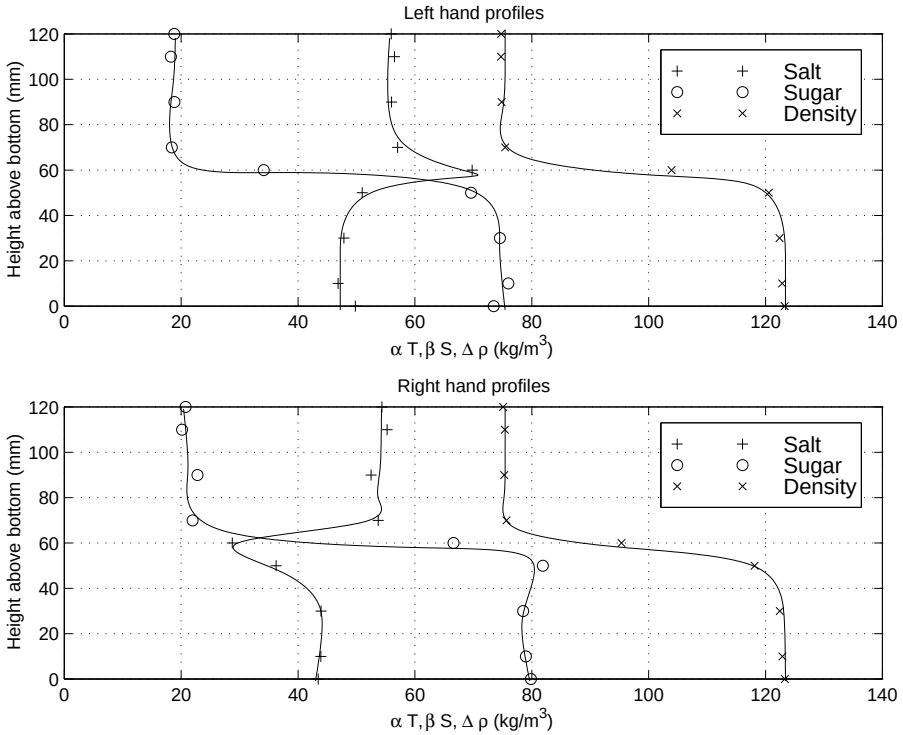

Figure 2: Sugar, salt and density profiles of the left and right hand side of the experimental tank. Salt and sugar concentrations are given in units of density

The steady state sugar, salinity and density profiles are shown in Figure 2. There are distinct differences between the left and right hand side of the tank, as would be expected from the antisymmetric convective patterns, so they are profiled separately. The most dominant feature of the profiles is the rapid increase of density at mid height. In particular, in both the left and right hand sides of the tank most of this increase has arisen from the sugar having settled predominantly to the bottom half of the tank. In contrast, the salt is marginally unstable in both sides of the tank, having slightly higher concentrations in the top half than in the bottom, and rapidly changing extrema at mid height.

Looking more carefully at the profiles, we can broadly divide each side of the tank into 4 layers. Starting with the left hand side, on top we have fairly constant concentrations for about 50mm. As mentioned earlier, fingers were observed in this region, which in this experiment are associated with a stable salt gradient, and an unstable sugar gradient. There are some indications of these gradients, although they are clearly very small compared to most of the other features.

The next 10mm contain rapid increases of both salt and sugar, thus leading to a very stable density profile. This acts as a very strong barrier to any kind of vertical convection through this layer, and indeed one would only expect pure diffusion to transfer properties from one side to the other. Measurements of the profile from Figure 2 leads us to estimates of the diffusive salt flux to be of order 0.14 mg/s, while the sugar flux is about 0.06mg/s. The rate at which both salt and sugar are being pumped into the tank through the source is approximately 8.33 mg/s, or about 60 and 150 times larger than the pure salt and sugar diffusive fluxes respectively.

From 50-60mm above the bottom of the tank there is a very stable sugar gradient, and an unstable salt gradient. We associate this with a strong diffusive layer, and indeed that is what is seen in the experiment. In the lowest 50 mm the sugar concentration gently increases and the salt decreases downward as in the diffusive layer above.

The layers are reversed in the right hand side of the tank. There is a region of weak diffusing layers on top of a sharp diffusive interface, followed by a layer stable in both properties, while weak fingering occurs in the lowest layer. The level of the sources and sink corresponds very closely to the interface between the strong diffusive layer and the stable layer.

As mentioned earlier, the dominant feature of the profiles was the fact that most of the sugar was in the bottom half of the tank, while the salt is marginally unstable. This is very similar to the profile one would expect if one had run a diffusive layer experiment by placing a salt solution above a sugar one. The unstable salt stratification drives the diffusive layers until the salt is nearly evenly distributed between the upper and lower halves, in the process raising some of the sugar, but not as much as the salt that is lowered. Diffusive layers do a better job of reducing the potential energy of a fluid than do fingers, so from energy considerations it is not surprising that the density field resembles that of a diffusive layers experiment rather than a fingers experiment. But given that both diffusive layers and fingers are active in this experiment, it is not immediately clear from a dynamic viewpoint as to why the diffusive layers dominate the concentration profiles.

Given that the sugar travels upwards through the diffusive layers, and downwards through the fingers, we present Figure 3 as a simplistic picture of the salt and sugar pathways through the tank.

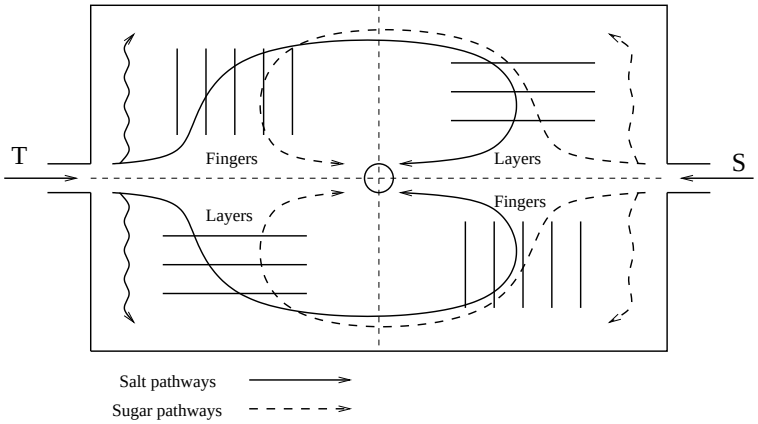

Figure 3: Simplistic picture of salt and sugar pathways through tank.

One aspect of double diffusion experiments that has been looked at quite closely is the ratio of the fluxes through either the fingers or the diffusive layers. For salt-sugar fingers the ratio of sugar to salt fluxes is around 0.9, provided the density ratio, $R_\rho = \alpha\bar{T}_z/\beta\bar{S}_z$ is not too close to one. For salt-sugar diffusive layers, the ratio of salt to sugar fluxes is around 0.6, again provided the density ratio is not too close to one. Given that we have four dominant flux pathways indicated in Figure 3, and four diffusive regions, we may construct a series of 4 equations with 4 unknowns. Alas, the 4 equations are not independent, nor are they even consistent, so there is no solution other than the trivial zero solution. We may illustrate this through an analogy with two connected water wheels. One water wheel is powered by a descending sugar solution, and it in turn raises a salt solution. There is friction in the system, so that it can only raise 9 kg of salt for every 10kg of sugar that falls through it. We shall call this the finger wheel. The second water wheel is powered by the descending salt solution, power it uses to raise the sugar solution. This water wheel has a greater friction, so that it can only raise 6kg of sugar for every 10kg of salt that powers it. This wheel is called the diffusive wheel. The two wheels are connected so that the salt raised by the finger wheel powers the diffusive interface wheel, which in turn raises the sugar to drive the first wheel. As the wheels are not 100% efficient, the system slows to a halt. Clearly we need some other mechanism to get either salt or sugar or both to the top of the system to drive the interconnected components so that they run continuously.

Figure 3 hints at one possibility. In the early stages of the experiment, while the tank was still close to being homogeneous, the plumes rapidly split into a core and sheath, one part rising up to the top of the tank, and the other half descending to the bottom. These are represented by the wiggly lines in Figure 3. In the final steady state, this process is not nearly as obvious, but never-the-less there are possible signs of it still occurring. Another option is the fact that most of the diffusive layers are inclined at an angle. This can be explained through the experimental evidence that fluid is moving parallel to these interfaces. Fluid immediately underneath the diffusive layer is continually getting denser, and so as it moves laterally underneath the interface, it also tends to sink, thus causing the interface to slope downwards. The fluid above the interface is continually getting lighter, thus it

must be moving in the opposite direction to the fluid underneath the interface so that in its direction of motion the interface is sloping upwards to accommodate its increased buoyancy. This advection can transport sugar or salt vertically (as it travels horizontally), without ever crossing the diffusive layer and thus being constrained to the flux transport ratios.

3 Theory

Before delving into the theory of diffusive fingers and layers, let us continue with the coupled water wheels analogy. For the wheels to turn, we require an additional driving force to overcome the friction of the system. Let us derive a formula for the ratio of the flux of the driving to the flux transport of the wheels.

Let us define F_{T1} to be the salt flux indicated in figure 3 for the path that travels from the source, up through the fingers, down through the layers, and then out through the outlet. F_{S1} is the corresponding value for the sugar flux. The two wiggly lines flowing upwards from the sources represent the driving terms F_{T2} and F_{S2}. The driving salt flux F_{T2} bypasses the fingers, using a different mechanism to get to the top, but then joins up with the salt flux F_{T1} in traveling down through the layers. Similarly, the driving sugar flux F_{S2} bypasses the layers, but joins up with F_{S1} to pass through the fingers. Let $\gamma_f \approx 0.9$ be the ratio of the sugar to salt flux through the fingers, and $\gamma_d \approx 0.6$ be the ratio of the salt to sugar flux through the diffusive layers. Thus we have the following relationships:

$$\frac{F_{T1}}{F_{S1}+F_{S2}} = \gamma_f, \quad \frac{F_{S1}}{F_{T1}+F_{T2}} = \gamma_d. \tag{1}$$

We rearrange to get

$$F_{T1} = \frac{\gamma_f(F_{S2}+\gamma_d F_{T2})}{1-\gamma_d\gamma_f}, \quad F_{S1} = \frac{\gamma_d(F_{T2}+\gamma_f F_{S2})}{1-\gamma_d\gamma_f} \tag{2}$$

We consider three situations.

- $F_{T2} = 0$:
$$\frac{F_{T1}}{F_{S2}} = \frac{\gamma_f}{1-\gamma_d\gamma_f} \approx 2.0, \quad \frac{F_{S1}}{F_{S2}} = \frac{\gamma_f\gamma_d}{1-\gamma_d\gamma_f} \approx 1.2 \tag{3}$$
- $F_{S2} = 0$:
$$\frac{F_{T1}}{F_{T2}} = \frac{\gamma_f\gamma_d}{1-\gamma_d\gamma_f} \approx 1.2, \quad \frac{F_{S1}}{F_{T2}} = \frac{\gamma_d}{1-\gamma_d\gamma_f} \approx 1.3 \tag{4}$$
- $F_{T2} = F_{S2}$:
$$\frac{F_{T1}}{F_{T2}+F_{S2}} = \frac{\gamma_f(1+\gamma_d)}{2(1-\gamma_d\gamma_f)} \approx 1.6, \quad \frac{F_{S1}}{F_{T2}+F_{S2}} = \frac{\gamma_d(1+\gamma_f)}{2(1-\gamma_d\gamma_f)} \approx 1.2. \tag{5}$$

It is clear that in all situations, the driving flux is able to generate more convection than itself in the fingers - diffusive layers system; however the ratio is not more than about two.

3.1 Salt Fingers

The linear stability analysis of the perturbations that grow into salt fingers is a well-studied problem, and reveals the wavelength of the disturbance which grows fastest. There remains some debate as to whether in the equilibrium model the fingers remain with this width (as proposed by Schmitt [3]), or whether they obtain a different width which maximises the buoyancy flux (see Stern [4] and Howard and Veronis [5]). Most theories appear to agree that the salt flux through fingers scales as the formula

$$\beta F_S \sim \frac{\kappa_T (\beta \Delta S)^2}{\alpha \bar{T}_z L^2} \tag{6}$$

where L is the buoyancy-layer scale defined as

$$L = \left(\frac{4\nu\kappa_T}{g\alpha \bar{T}_z} \right)^{1/4}. \tag{7}$$

The discrepancy between most formulas comes into the formula for $\bar{T}_z$. It is the unstable salt field which drives the fingers, and thus presumably controls the gradients in the finger zone, so ideally one would like to rewrite the temperature gradient T_z that appears in (6) in terms of the salinity difference in order to determine the flux law solely as a function of $\beta\Delta S$. Many people favour a 4/3 power law (see Stern [4], section 11.4), and there is experimental evidence in support of this (Turner [6]). However, as we have profiles of both the T and S field, we are able to try either formula, and see if they give consistent results. The formula we shall use is that derived by Howard and Veronis [5] in the form of (6) given by

$$\beta F_{S1} = 0.1578 \sqrt{\frac{g\kappa_t}{\nu}} \; \frac{(\beta\Delta S)^2}{\sqrt{\bar{T}_z}}, \tag{8}$$

together with Stern and Turner's [7] empirically fit curve to the 4/3 power law

$$\beta F_{S2} = C(\beta \Delta S)^{4/3}, \tag{9}$$

where $C = 10^{-4}$ m/s

In both cases we assume the heat flux F_T is a factor of 0.91 [7] times the salt flux.

3.2 Diffusive Layers

Turner [8] first suggested that since convection through diffusive layers was similar to Rayleigh Bénard convection, the formula for the heat flux should scale in a similar fashion. That is, the nondimensional heat flux through diffusive layers, given by the Nusselt number, $Nu_T = F_T d/\kappa_T \Delta T$, should be proportional to the Rayleigh number to the power of 1/3. The reasoning behind this relationship is that the length scale of the convective rolls is not in general governed by the size of the tank, and it is this relationship that removes the external length scale dependence. It follows that the heat flux is given by

$$\alpha F_T = C(R_\rho) \, (g\kappa_T^2/\nu)^{1/3} \, (\alpha \Delta T)^{4/3} \tag{10}$$

1:Fingers	5:W. Diffusion
2:Stable	6:S. Diffusion
3:S. Diffusion	7:Stable
4:W. Diffusion	8:Fingers

Figure 4: The geometry of the 8 Box model

The function C has quite a strong dependence on R_ρ, especially for heat salt systems. Shirtcliffe [9] found his experimental results fit the formula

$$C = 2.6 R_\rho^{-12.6}. \tag{11}$$

He also provided an estimate for the flux ratio, $\beta F_S / \alpha F_T = 0.60$.

4 The Flux box model

As mentioned previously in section 2, the experimental profiles drawn in Figure 2 suggest the tank can be divided up into eight primary regions, four on each side. We draw them in Figure 4.

Table 1 provides all the data necessary to solve the flux equations given in the preceding section. To get the total flux of either solute, we must multiply by the area of the region where the fingering or diffusive layer is present. We assume this area is constant for all six of the interfaces we consider, and non-dimensionalise it by half the actual physical area of the box A, writing the non-dimensional area by A_f. We then non-dimensionalise the fluxes by the input salt and sugar flux, and the answers are listed in Table 1.

One clear result is that the flux through box 1 is much smaller than any of the other fluxes. This results from the extremely small unstable sugar gradient which is driving it. There is a large amount of uncertainty in the value for $\beta \Delta S$, indeed it may be up to a factor of three bigger than the best fitting line used to generate the value listed. This would increase the values of F_{S1} and F_{T1} by a factor of 9, but they would still remain negligible compared to the other terms.

Another clear result is that nearly all the fluxes are much larger than physically reasonable. Although we have not substituted in a value for A_f, we would expect it to be of order one, meaning that the entire left hand of the tank is fingering in the top layer, diffusing in the bottom, and vice-versa in the right hand side. The dimensionless flux values listed imply the dimensional fluxes are often over 100 times greater than the input flux. Referring to our previous water wheel analogy, a small amount of driving can generate fluxes through

Property	Box 1	Box 2	Box 3	Box 4	Box 5	Box 6	Box 7	Box 8
height (m)	0.05	0.01	0.01	0.03	0.05	0.01	0.01	0.03
$\alpha\Delta T$	0.8	13.2	-19	-4	-1.4	-24.2	7	8
$\beta\Delta S$	-0.13	15.5	36	6	1.9	44.6	15	-3.5
R_ρ	6	-	1.9	1.5	1.4	1.8	-	2.3
$\alpha\bar{T}_z(m^{-1})$	16	1320	-1900	-133	-28	-2420	700	-267
$\alpha F^*_{S1}/A_f$	0.7	-	-	-	-	-	-	130
$\alpha F^*_{T1}/A_f$	0.6	-	-	-	-	-	-	110
$\alpha F^*_{S2}/A_f$	0.015	-	-	-	-	-	-	11
$\alpha F^*_{T2}/A_f$	0.013	-	-	-	-	-	-	9.7
$\alpha F^*_{S3}/A_f$	-	-	54	130	110	20	-	-
$\alpha F^*_{T3}/A_f$	-	-	90	210	190	34	-	-

Table 1: Properties of the Eight Boxes. The fluxes have been normalised by the source input fluxes. A_f is the area of the convecting region divided by the area of half the tank. The subscripts on the fluxes refer to whether they were predicted by equation (8), (9) or (10) respectively.

the coupled diffusive system greater than the driving term, but by no more than a factor of two. Clearly a factor of 100 or more is out of the question, even if it were possible for the entire input fluxes to reach the top of the tank by some unidentified mechanism to become the driving flux. Thus there must be a problem with our application of the theory. There are a few obvious suggestions. Firstly, the formula by Howard and Veronis was derived for two fluids which have vastly different diffusivities. It was designed for the heat-salt system rather than our sugar-salt system. They allowed the salt to pass through the fingers without diffusing, so one would expect their formula to predict a larger salt flux than the sugar-salt experiment produces. Secondly, our profiles of the both the sugar and salt in most cases just do not have the resolution required to gain accurate values of the salt and sugar contrasts across the interfaces. The contrasts that appear in the theories refer to the contrasts that occur across the finger or layer interfaces, while we are using instead the contrasts that occur across the whole box. In the one dimensional theories the fluid above and below the interfaces are usually well mixed, so this difference is not important. In our experiment, the regions are distinctly two dimensional. This is most obvious in the experiment through the observation that the diffusive layers are generally inclined at some angle to the horizontal. This slope is associated with advection parallel to the interface, and we seem not to have the well mixed regions above and below the interfaces that the theories assume. Thus the difference between the sugar or salt contrasts across the interfaces, and the corresponding differences across the boxes that we used to apply the theories may be significant. To conclude, we suggest that the simple theories derived from one dimensional models do not adequately describe this complicated two dimensional system.

5 The box model

In the previous section, we divided the tank up into the eight well defined regions observed in Figure 2. In that model, we used the temperatures and salinities found on the boundary of the boxes to determine the fluxes within each box. Let us now construct a similar box model corresponding to those eight regions, but now assign a mean temperature and salinity to each box rather than boundary values. The idea in this model is to try to calculate the fluxes between the boxes as opposed to the fluxes within each box.

In the previous section, we found that the simple one dimensional formulas for fingering and diffusion did not adequately describe the experimental system. Let us discard these theories and return to the simple assumption that the flux between two boxes is proportional to the difference in concentration between those boxes. Writing a formula for the rate of change of salinity in box 1, we get

$$V_1\dot{T_1} = b_{12}(T_2 - T_1) + b_{15}(T_5 - T_1) + T_{i1}C - Q_1T_1 \equiv 0. \tag{12}$$

The final equivalence is due to the fact that we are interested in finding the steady state solution. The first two terms on the right hand side of this equation are the fluxes of sugar into box 1 from box 2 and box 5 respectively, where the b terms are unknown flux transfer coefficients. The third term represents a source input term. For the moment we will assume that the salt source is able to directly inject fluid into all four boxes on the left hand side of the tank (boxes 1-4). C is the salinity of the salt source, also equal to the concentration of sugar in the sugar source, while T_{i1} is an unknown outflow coefficient. The fourth term represents the rate of outflow of salt from box 1, where Q_1 represents the rate at which fluid is leaving box 1, which has salinity T_1. Finally V_1 is the volume of box 1. We choose to use units of kg/m^3 for both salt and sugar concentrations, so the transfer coefficients b_{ij} have units of m^3/s. It is tempting to interpret these as the volume flux between box i and box j; however this is would only be correct if the flux transports were due to advection only, which is not true. To further emphasise this, we use different transfer co-efficients for the corresponding sugar equations, a_{ij}.

Inherent in the above equation is the assumption that each box is homogeneous. Thus, the flux of either solute to the outflow is equal to the the volume flux of the fluid leaving that box times the concentration of that solute. In addition, we assume that fluid entering each box from the inflow has the concentration of the reservoirs, and thus the flux of either salt is proportional to the volume flux times the concentration.

There are similar equations for rate of change of salinity for the remaining 7 boxes, as well as the 8 corresponding equations for sugar, and they may be found in the appendix. In addition, there are two more conservation equations. They are simply that the sum of the individual salt sources is equal to the flux of the salt source, $C\sum_j T_{ij} = QC$, as is the sum of the individual sugar sources, $C\sum_j S_{ij} = QC$. There are also two similar conservation equations for the sum of the outflow terms, however they are already implicitly expressed in the previous 18 equations.

The experimental data gives us the values of the sugar and salt concentrations in the boxes. Thus the unknowns are the 10 transfer parameters for each of sugar and salt, the 8 output flux terms Q_j, and the 4 input flux terms for each of salt and sugar - a total of 36

unknowns.

As of the moment, we have 19 equations - just over half the number of unknowns - a highly under-determined problem. We can introduce more equations, for example by relating the transfer coefficients in some way, or reducing the number of unknowns by restricting inflow and outflow from some boxes, but for the moment, let us discuss a method of finding solutions to under-determined problems, described by Veronis in General Ocean Circulation [10].

Our eighteen equations may be written in matrix form $\mathbf{Ax} = \mathbf{b}$. Here $\mathbf{A}$ has 19 rows and 36 columns, or more generally $m \times n$, where m is less than n. The sizes of $\mathbf{x}$ and $\mathbf{b}$ are $n \times 1$ and $m \times 1$ respectively.

The key to the method is to assume we can write $\mathbf{x} = \mathbf{A^T f}$, where $\mathbf{A^T}$ is the transpose of $\mathbf{A}$, and $\mathbf{f}$ is a yet to be determined matrix of size $m \times 1$. $\mathbf{f}$ satisfies the following equation, $\mathbf{AA^T f} = \mathbf{Ax} = \mathbf{b}$. Now $\mathbf{AA^T}$ is square $(m \times m)$, and if it has a non-zero determinant, we may solve for $\mathbf{f} = (\mathbf{AA^T})^{-1}\mathbf{b}$, and thus $\mathbf{x} = \mathbf{A^T}(\mathbf{AA^T})^{-1}\mathbf{b}$.

We have thus determined a unique solution to an undetermined problem. The apparent paradox is explained through the writing of $\mathbf{x} = \mathbf{A^T f}$. This means we are writing the solution vector $\mathbf{x}$ as a linear combination of the m vectors that make up the rows of $\mathbf{A}$. $\mathbf{x}$ has n components, and thus defines a point in an n dimensional space. We cannot write all the points in the n dimensional space through the summation of m vectors. It turns out that the solution this method returns is a projection of the (unknown) true solution in n dimensional space, onto a m dimensional space defined by the m rows of $\mathbf{A}$.

Let us take the example of $x+y = 10$, so $\mathbf{A}$=[1, 1]. We do not know what the true solution is, other than it lies on the line $y = 10-x$, but its projection onto the one dimensional vector space defined by the one row of $\mathbf{A}$ is $x = y = 5$. It is clear in the formulation of the problem that we have not treated x any differently to y, and that is reflected in the identical values returned. This is important, as if we distinguish between them somehow, then that can make a great difference. For example, let us non-dimensionalise x by L, and y by $2L$, writing $X = x/L$ and $Y = y/(2L)$. The original equation may now be written $X + 2Y = 10/L$, and the returned solution is $X = 2/L$, $Y = 4/L$, which lies on the space defined by the vector $(1, 2)$, the row of $\mathbf{A}$. In terms of the original variables, the solution is $x = 2$, $y = 8$, vastly different to the previous solution (5,5) even though the equation solved was identical. This has important consequences for how we scale our problem. We must choose consistent scales for all quantities, as otherwise the solution will be biased towards those quantities that were scaled by values too large. It is clear that to use this method, if there is no reason to favour any unknown value over any other, then it is important to reflect that in the formulation of the equations, so that their co-efficients are equal.

Figure 5 shows how the solutions to the box model equations do not change dramatically as we increase the number of equations until they equal the number of unknowns. Plotted are the inflow, outflow and cross box salt and sugar flux transports. The fluxes have been normalised so that the sum of each of the salt and sugar inflows is 100, as is the sum of each of the outflows. In picture (a), only the 19 equations listed in the appendix have been used. The main point to note in this picture is that the horizontal transports are an order of magnitude bigger than the vertical transports. In addition, the inflows and outflows to the two middle layers are also an order of magnitude larger than the corresponding values for the

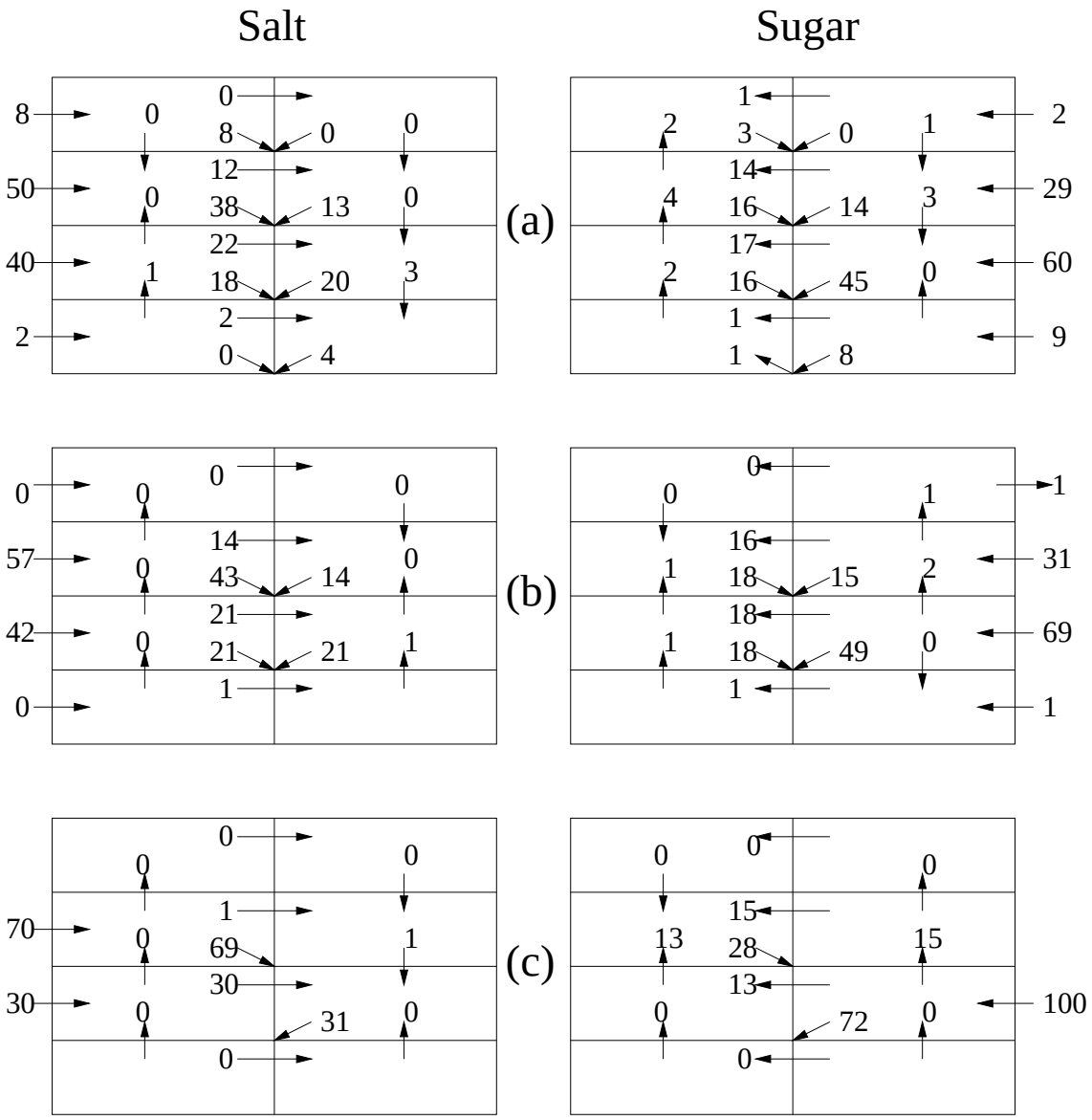

Figure 5: Salt and sugar fluxes given by the solution to the box model equations. The fluxes have been normalised so that the sum of each of the inflows is 100, as is the sum of the outflows. In (a), only the original 19 equations are solved. In (b), there are an additional 10 equations, corresponding to limiting the outflows to the middle two layers, and applying the six vertical dynamic constraints. (c) is an exact solution, as it contains the same number of unknowns as equations. It differs from (b) through the inflows being limited to the 3 boxes indicated, while the outflows have been limited further to just the two middle layers.

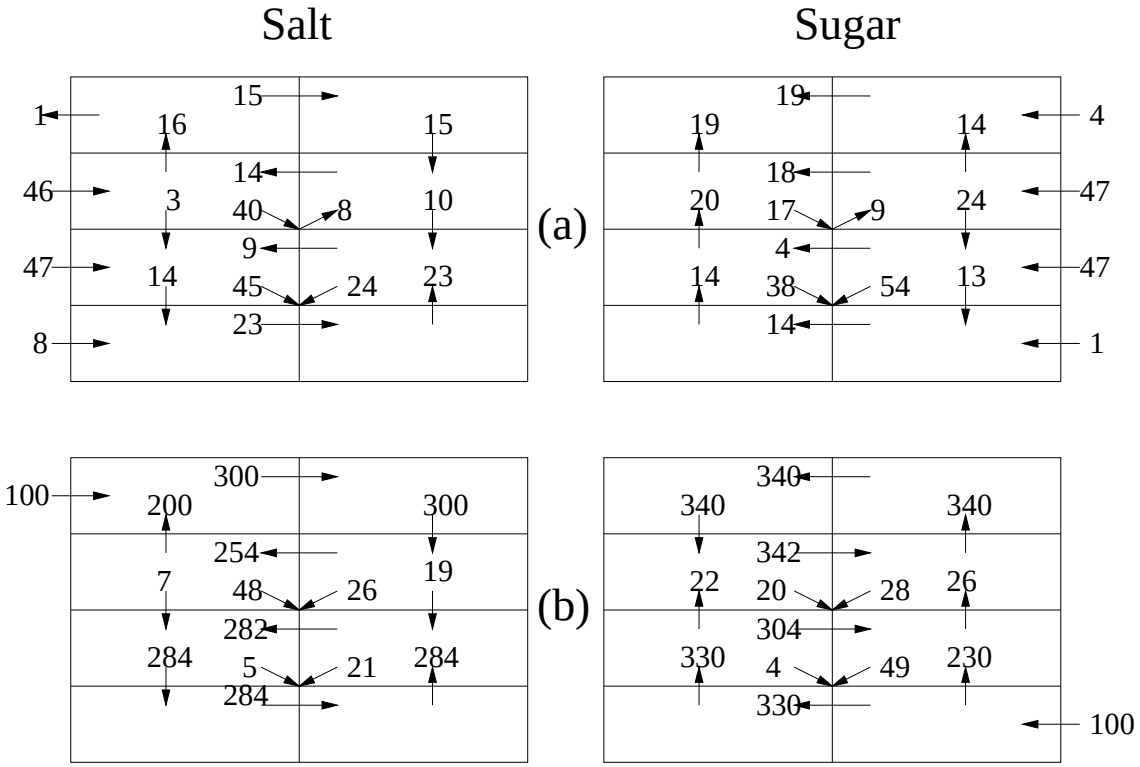

Figure 6: Fluxes of salt and sugar given by the solutions to the box model equations. Fluxes normalised as in figure 5. In (a), the coefficients of the inflows have been reduced from C_0 to $C_0/50$. In (b) the source inputs are limited to the top left and bottom right hand boxes. In both cases the outflows are limited to the middle two boxes on each side, and the six vertical dynamical constraints described in the text are applied.

upper and lower layer. As a result, there is very little transport of sugar or salt occurring in the upper and lower layers. In (b), there are an additional 10 constraints, consisting of restricting the outflow from 8 to four layers, and adding 6 vertical dynamical constraints. These are based on symmetry arguments and are $a_{12} = a_{78}$, $b_{12} = b_{78}$, $a_{23} = a_{67}$, $b_{23} = b_{67}$, $a_{34} = a_{56}$ and $b_{34} = b_{56}$. Notice the fluxes are very similar to those plotted in (a). In (c), the solution is exact, as the number of unknowns is the same as the number of equations. To achieve this match, we have had to restrict the inflows to just the 3 boxes indicated, and the outflows to the two boxes indicated. We feel these constraints are too harsh, and we provide the result only to show the the exact solution is not too dissimilar to those plotted in (a) and (b).

Our reason for the unexpectedly small fluxes in the upper and lower layers, particularly in Figure 5 (a) where we have not forbidden inflow or outflow to the top and bottom layers, is that we have formulated our original 19 equations in a manner that is biased against fluxes in these regions. This is due to assuming the input source enters all boxes at the source concentration. This is a reasonable assumption for the middle two layers, but not so for the upper and lower layers. The main reason for allowing inflow and outflow from the upper and lower layers is to allow some mechanism to drive the diffusive 'water wheels'. While we have not specified what that mechanism is, although we suspect it is due to vertical transport along the sloping diffusive layers, it is highly improbable that the flux from the source to the upper and lower layers via this mechanism arrives with the concentration of the inflow. We have seen in the examples provided earlier that if we non-dimensionalise a term in the under-determined system of equations by an large quantity, then that term dominates the equation. Thus we expect the inflow terms to dominate the equations. For conservation arguments, this term must be balanced by the sum of the other terms, and the co-efficient of the outflow is the next biggest term, so it is the next most dominant term. Thus we see the cross-box transport seems to play a minor role in these conservation equations.

To see how changing the scaling for the input terms makes a difference, in Figure 6 (a) we show the solution to the system of equations where the source term is now the source concentration divided by 50. We can see in this figure that the vertical fluxes is now a similar order of magnitude to the horizontal fluxes, and we have convection in the upper and lower layers. This solution matches nicely the schematic drawing of the fluxes drawn in Figure 3, however it is not realistic, as we should really only rescale the input terms to the upper and lower boxes in this way. If we were to do that however, we would somehow have to redistribute the lost concentration to the two middle layers, the method by which to do so is currently not clear.

As a final test of our box model, we try restricting the source terms to solely the upper left and lower right boxes. The resulting fluxes are pictured in Figure 6 (b). Notice the very large recirculations apparent in the upper and lower halves. This bears a nice similarity to the water-wheel analogy. A driving flux can generate larger fluxes in the coupled double diffusive regions that the driving flux itself. In this case the factor is greater than the maximum factor of two predicted by the theory, but we have not specified any flux ratio parameters for the finger or diffusive regions, and thus we would not expect a match. This example also helps to explain why we see very little inflow or outflow from the upper or lower layers. It does not take much of an inflow in these layers to drive large amounts of recirculation in the middle

layers. It seems logical that this model tends to reject these high-energy solutions when there is a much simpler solution with no flux in the upper and lower layers.

6 Conclusion

We have seen that a coupled system of fingers and diffusive layers cannot be sustained adjacent to each other without some other driving mechanism to transport either salt or sugar to the top of system. With driving, the resulting fluxes through the fingers and diffusive layers can be up to twice as large as the original driving term.

The one dimensional flux laws predict fluxes through the salt fingers and diffusive layers up to a few hundred times the source fluxes. These are much too large to be considered possible. While the flux laws used are not without question, it is more likely that the two dimensional problem we are analysing is too far removed from the one-dimensional theories to be of use, in addition to the experimental data being a little too sparsely separated.

Our box model only permits the driving flux to enter the top of the system at the same concentration as the source. The large co-efficient of this source term dominates the vector space of the possible solution set, and to first order it is the outflow that matches this term. The cross box transports play only a minor role in the solutions. Small amounts of source flux terms in the upper and lower layers produce large amounts of recirculation in the middle layers, which the model rejects in favour of the less energetic solutions that contain very little input terms to the upper and lower layers. To generate non-negligible amounts of convection in the upper and lower layers, we require a theory for the mechanism behind the driving term, which we may then use to scale the source terms for the upper and lower layers.

7 Acknowledgements

I would like to thank George Veronis greatly for his endless patience in guiding me through this project, for introducing us to the wonderful game that is social softball, and for some wonderful evenings enjoying life at Crooked Pond (thanks also Kim). Thanks also to Stuart Turner for his help during the two weeks he was here, in addition to dreaming up and carrying out the original experiment, and for providing me with the experimental results.

A very special thank you to all the other fellows who helped to make this summer so enjoyable (perhaps more than it was supposed to be): Roberto, Pascale, Jen, Nifer, Jeff, Meredith, Yuan-Nan and Raffaele. In addition, thanks to the pseudo-fellows who went above and beyond their call of duty in keeping us smiling: Claudia Pasquero, Jean-Luc Thiffeault, Allison Moehlis, Stephan Llewellyn Smith and Francesco Paparella.

Finally, thanks to Neil Balmforth for not visibly regretting the decision to invite me in the first place.

8 Appendix: The box model equations

The model has nineteen basic equations, comprised of a sugar equation for each box,

$$\dot{S}_1 = a_{12}(S_2 - S_1) + a_{15}(S_5 - S_1) + CS_{i1} - S_1Q_1 \equiv 0,$$

$$\dot{S}_2 = a_{12}(S_1 - S_2) + a_{23}(S_3 - S_2) + a_{26}(S_6 - S_2) + CS_{i2} - S_2Q_2 \equiv 0,$$

$$\dot{S}_3 = a_{23}(S_2 - S_3) + a_{34}(S_4 - S_3) + a_{37}(S_7 - S_3) + CS_{i3} - S_3Q_3 \equiv 0,$$

$$\dot{S}_4 = a_{34}(S_3 - S_4) + a_{48}(S_8 - S_4) + CS_{i4} - S_4Q_4 \equiv 0,$$

$$\dot{S}_5 = a_{15}(S_1 - S_5) + a_{56}(S_6 - S_5) - S_5Q_5 \equiv 0,$$

$$\dot{S}_6 = a_{26}(S_2 - S_6) + a_{56}(S_5 - S_6) + a_{67}(S_7 - S_6) - S_6Q_6 \equiv 0,$$

$$\dot{S}_7 = a_{37}(S_3 - S_7) + a_{67}(S_6 - S_7) + a_{78}(S_8 - S_7) - S_7Q_7 \equiv 0,$$

$$\dot{S}_8 = a_{48}(S_4 - S_8) + a_{78}(S_7 - S_8) - S_8Q_8 \equiv 0,$$

a salt equation for each box,

$$\dot{T}_1 = b_{12}(T_2 - T_1) + b_{15}(T_5 - T_1) - T_1Q_1 \equiv 0,$$

$$\dot{T}_2 = b_{12}(T_1 - T_2) + b_{23}(T_3 - T_2) + b_{26}(T_6 - T_2) - T_2Q_2 \equiv 0,$$

$$\dot{T}_3 = b_{23}(T_2 - T_3) + b_{34}(T_4 - T_3) + b_{37}(T_7 - T_3) - T_3Q_3 \equiv 0,$$

$$\dot{T}_4 = b_{34}(T_3 - T_4) + b_{48}(T_8 - T_4) - T_4Q_4 \equiv 0,$$

$$\dot{T}_5 = b_{15}(T_1 - T_5) + b_{56}(T_6 - T_5) + CT_{i5} - T_5Q_5 \equiv 0,$$

$$\dot{T}_6 = b_{26}(T_2 - T_6) + b_{56}(T_5 - T_6) + b_{67}(T_7 - T_6) + CT_{i6} - T_6Q_6 \equiv 0,$$

$$\dot{T}_7 = b_{37}(T_3 - T_7) + b_{67}(T_6 - T_7) + b_{78}(T_8 - T_7) + CT_{i7} - T_7Q_7 \equiv 0,$$

$$\dot{T}_8 = b_{48}(T_4 - T_8) + b_{78}(T_7 - T_8) + CT_{i8} - T_8Q_8 \equiv 0,$$

plus three conservation equations,

$$Q_1 + Q_2 + Q_3 + Q_4 + Q_5 + Q_6 + Q_7 + Q_8 = 2Q,$$

$$S_{i1} + S_{i2} + S_{i3} + S_{i4} = Q,$$

$$T_{i1} + T_{i2} + T_{i3} + T_{i4} = Q.$$

References

[1] M. Stern, "The 'salt fountain' and thermohaline convection," Tellus **12**, 172 (1960).

[2] H. Stommel, A. Arons, and D. Blanchard, "An oceanongraphical curiosity: The perpetual salt fountain," Deep-Sea Res. **3**, 152 (1956).

[3] R. Schmitt, "The growth rate of super-critical salt fingers," Deep-Sea Res. **26**, 23 (1979).

[4] M. Stern, *Ocean Circulation Physics* (Academic, London, 1975).

[5] L. Howard and G. Veronis, "The salt-finger zone," J. Mar. Res. **3**, 265 (1948).

[6] J. Turner, "Salt fingers across a density interface," Deep-Sea Res. **14**, 599 (1967).

[7] M. Stern and J. Turner, "Salt fingers and convecting layers," Deep-Sea Res. **16**, 497 (1969).

[8] J. Turner, "The couple turbulent transports of salt and heat across a sharp density interface," Int. J. Heat Mass Tranfer **8**, 759 (1965).

[9] T. Shirtcliffe, "Double diffusive convection with similar diffusivities," J. Fluid Mech. **57**, 27 (1973).

[10] *General Circulation of the Ocean*, edited by H. Abarbanel and W. Young (Springer-Verlag, New York, 1987).